AMERICAN SOCIETY FOR MICROBIOLOGY | Journal of Virology®

VIRUS-CELL INTERACTIONS

Type I Interferon Acts as a Major Barrier to the Establishment of Persistent Infectious Bursal Disease Virus Infections

Laura Broto,[a] Nicolás Romero,[a]* Fernando Méndez,[a] Elisabet Diaz-Beneitez,[a] Oscar Candelas-Rivera,[a] Daniel Fuentes,[a] Liliana L. Cubas-Gaona,[a]* Céline Courtillon,[b] Nicolas Eterradossi,[b] Sébastien M. Soubies,[b] Juan R. Rodríguez,[a] Dolores Rodríguez,[a] José F. Rodríguez[a]

[a]Departamento de Biología Molecular y Celular, Centro Nacional de Biotecnología-CSIC, Madrid, Spain

[b]OIE Reference Laboratory for Gumboro Disease, Avian and Rabbit Virology, Immunology and Parasitology Unit (VIPAC), French Agency for Food, Environmental and Occupational Health Safety (ANSES), Ploufragan, France

Laura Broto, Nicolás Romero, and Fernando Méndez contributed equally to this work. Author order was determined by consensus among them.

ABSTRACT Infectious bursal disease virus (IBDV), the best-characterized member of the *Birnaviridae* family, is a highly relevant avian pathogen causing both acute and persistent infections in different avian hosts. Here, we describe the establishment of clonal, long-term, productive persistent IBDV infections in DF-1 chicken embryonic fibroblasts. Although virus yields in persistently infected cells are exceedingly lower than those detected in acutely infected cells, the replication fitness of viruses isolated from persistently infected cells is higher than that of the parental virus. Persistently infected DF-1 and IBDV-cured cell lines derived from them do not respond to type I interferon (IFN). High-throughput genome sequencing revealed that this defect is due to mutations affecting the IFN-α/β receptor subunit 2 (IFNAR2) gene, resulting in the expression of IFNAR2 polypeptides harboring large C-terminal deletions that abolish the signaling capacity of IFN-α/β receptor complex. Ectopic expression of a recombinant chicken IFNAR2 gene efficiently rescues IFN-α responsiveness. IBDV-cured cell lines derived from persistently infected cells exhibit a drastically enhanced susceptibility to establishing new persistent IBDV infections. Additionally, experiments carried out with human HeLa cells lacking the IFNAR2 gene fully recapitulate results obtained with DF-1 cells, exhibiting a highly enhanced capacity to both survive the acute IBDV infection phase and to support the establishment of persistent IBDV infections. Results presented here show that the inactivation of the JAK-STAT signaling pathway significantly reduces the apoptotic response induced by the infection, facilitating the establishment and maintenance of IBDV persistent infections.

IMPORTANCE Members of the *Birnaviridae* family, including infectious bursal disease virus (IBDV), exhibit a dual behavior, causing acute infections that are often followed by the establishment of lifelong persistent asymptomatic infections. Indeed, persistently infected specimens might act as efficient virus reservoirs, potentially contributing to virus dissemination. Despite the key importance of this biological trait, information about mechanisms triggering IBDV persistency is negligible. Our report evidences the capacity of IBDV, a highly relevant avian pathogen, to establish long-term, productive, persistent infections in both avian and human cell lines. Data presented here provide novel and direct evidence about the crucial role of type I IFNs on the fate of IBDV-infected cells and their contribution to controlling the establishment of IBDV persistent infections. The use of cell lines unable to respond to type I IFNs opens a promising venue to unveiling additional factors contributing to IBDV persistency.

KEYWORDS IFNAR2, apoptosis, birnavirus, double-stranded RNA virus, infectious bursal disease virus, interferons, persistent infection

Citation Broto L, Romero N, Méndez F, Diaz-Beneitez E, Candelas-Rivera O, Fuentes D, Cubas-Gaona LL, Courtillon C, Eterradossi N, Soubies SM, Rodríguez JR, Rodríguez D, Rodríguez JF. 2021. Type I interferon acts as a major barrier to the establishment of persistent infectious bursal disease virus infections. J Virol 95:e02017-20. https://doi.org/10.1128/JVI.02017-20.

Editor Susana López, Instituto de Biotecnologia/UNAM

Address correspondence to José F. Rodríguez, jfrodrig@cnb.csic.es.

* Present address: Nicolás Romero, Department of Virology, Parasitology and Immunology, Faculty of Veterinary Medicine, Ghent University, Ghent, Belgium; Liliana L. Cubas-Gaona, OIE Reference Laboratory for Gumboro Disease, Avian and Rabbit Virology, Immunology and Parasitology Unit (VIPAC), French Agency for Food, Environmental and Occupational Health Safety (ANSES), Ploufragan, France.

Received 13 October 2020
Accepted 4 December 2020
Accepted manuscript posted online 16 December 2020
Published 10 February 2021

Viruses are obligate intracellular pathogens establishing complex relationships with their hosts to successfully accomplish their main biological roles, i.e., replicating and spreading. Most viruses cause short-lived acute infections ensuring the production of an abundant infective progeny. This enables virus dissemination before the host's immune system clears the infection. As a general rule, viruses exploiting this strategy are cytocidal. However, under certain circumstances, some lytic viruses, e.g., reoviruses and picornaviruses, deviate from this behavior and establish productive persistent infections in their hosts and/or in cultured cells (1, 2).

Members of the *Birnaviridae* family (3) also exhibit a dual behavior, causing acute infections that are often followed by the establishment of lifelong persistency. Epitomizing the major biological significance of this trait, birnaviruses belonging to all four family genera have been isolated from asymptomatic carrier specimens, including insects (4), fish (5, 6), and birds (reviewed in reference 7). In addition, several reports have described the detection of RNA and infectious bursal disease virus (IBDV) in tissues collected from experimentally infected chickens long after the vanishing of clinical signs of disease (8–10). Despite this, the characterization of the molecular basis underlying the initiation and maintenance of birnaviral persistent infections has been customarily overlooked. Hence, current information about this key biological feature, largely shaping birnavirus lifestyles, is rather scarce.

IBDV, the sole member of the *Avibirnavirus* genus, is the best-characterized component of the *Birnaviridae* family. IBDV virions are naked icosahedrons (65 to 70 nm in diameter; T = 13L symmetry) harboring a single capsid enclosing a bipartite double-stranded RNA genome that encodes five mature polypeptides (VP1 to VP5) (7).

Although productively infecting a wide variety of bird species, clinical signs of disease have only been reported in juvenile (2 to 6 weeks old) domestic chickens (*Gallus gallus*). Two IBDV serotypes have been identified thus far. Serotype II strains, mainly isolated from asymptomatic turkeys (*Maleagris gallopavo*), are nonpathogenic for chickens. In contrast, all serotype I strains induce clinical signs of disease. However, the virulence of these strains is highly variable, ranging from mild to very virulent, with the latter causing very high (nearing 100%) mortality rates in unvaccinated chicken flocks. Indeed, very virulent IBDV strains pose a major threat to the poultry industry worldwide (reviewed in reference 11).

Several years ago, our group described the establishment of IBDV persistent infections in chicken DT40 cultured cells (12). Regrettably, DT40 cells originated from a chicken lymphoma, hence, *ab initio* being persistently infected with avian leukosis virus (ALV) (13). Indeed, the presence of coinfecting ALV posed a major obstacle to studying the mechanism(s) allowing the establishment of IBDV persistent infections.

Here, we describe an experimental model allowing us to generate long-term, stable, persistent IBDV infections in chicken DF-1 and human HeLa cells, both free of endogenous viruses.

Our results show that IBDV infection involves an acute phase characterized by very active virus replication, the release of high virus titers, and a massive apoptotic response that kills most infected cells. Cells surviving the initial acute phase remain persistently infected, sustaining cell proliferation while enduring highly mitigated virus replication. The long-term maintenance of persistently infected DF-1 cells leads to the selection of clonal cell populations unable to respond to type I interferon (IFN).

Data collected after the pharmacological elimination of IBDV from persistently infected cells indicate that the functional inactivation of type I IFN signaling drastically increases both the capacity of infected cells to survive the acute IBDV infection phase and their susceptibility to establishing new persistent infections. Work carried out with a knockout human HeLa cell line unable to respond to type I IFN fully recapitulates data gathered with chicken DF-1 cells.

This report provides a novel molecular insight about the crucial role of type I IFNs in the fate of IBDV-infected cells and their contribution to controlling the establishment of IBDV persistent infections.

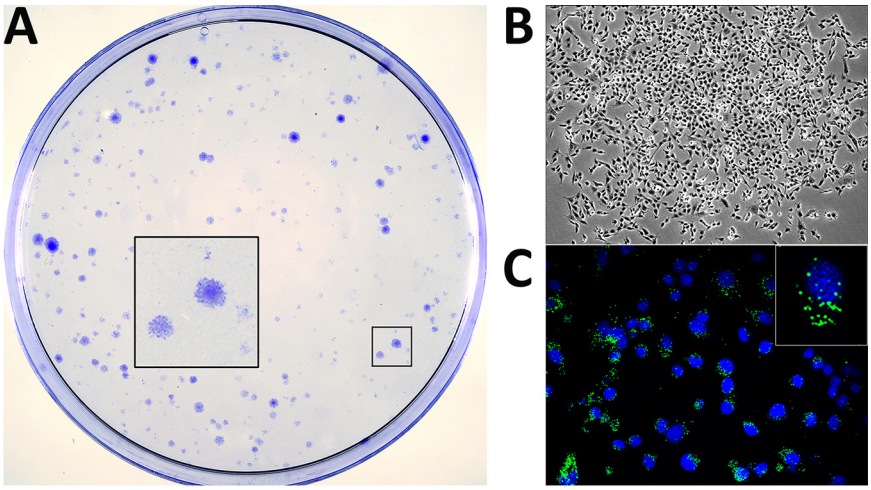

FIG 1 Generation of persistently infected DF-1 cell cultures. DF-1 cell monolayers were infected with IBDV at an MOI of 3 PFU/cell. At 4 days p.i., cultures were carefully rinsed to remove cell debris and then maintained in DMEM supplemented with 10% FCS. Culture medium was replaced every 5 days. At 21 days p.i., cultures were either stained with crystal violet to visualize surviving cell clones (A) or processed for phase-contrast (B) or IF (C) microscopy after incubation with an antibody specifically recognizing the IBDV structural VP3 polypeptide (green). Cell nuclei (blue) were stained with DAPI. Insets show a higher magnification (×2.5) of boxed areas.

RESULTS

Establishment of IBDV persistent infections. Infection of DF-1 cell monolayers with IBDV invariably leads to massive cell death within the first 48 to 72 h postinfection (p.i.). However, a marginal fraction of infected cells remains alive long after this period. This recurrent observation led us to perform a detailed characterization of this phenomenon.

Preconfluent DF-1 monolayers were infected at a multiplicity of infection (MOI) of 3 PFU per cell with IBDV. Four days later, culture plates were rinsed twice with DMEM to remove cell debris and then maintained in normal medium. Cell culture medium was routinely replaced every 5 days. After 3 weeks, cultures were either stained with crystal violet to visualize surviving cells or processed for immunofluorescence (IF) to assess the expression of the virus-encoded VP3 polypeptide.

As shown in Fig. 1A, after the 21-day recovery period, culture plates were populated with well-differentiated cell islets exhibiting a wide size range. Microscopic analysis indicated that, regardless of their size, islets were formed by healthy-looking cells (Fig. 1B) showing a specific VP3 IF signal formed by discrete protein accumulations within the perinuclear region (Fig. 1C). Indeed, VP3 expression indicated that cell islets were formed by persistently infected cells. These cultures are termed persistently infected DF-1 (DF-1P).

Assuming the clonal origin of these cell islets and considering the number of them versus the initial number of infected cells in the plates, data gathered from three independent experiments indicate that 0.023% $\pm$ 0.007% of the infected DF-1 cell population survives the acute IBDV infection phase.

It is worth noting that during the first two to three months, DF-1P cultures undergo sporadic crises resulting in the death of a substantial fraction of the total cell population. However, after this period, cultures become stable, maintaining steady proliferation rates.

Characterization of DF-1P cultures. Three independently generated DF-1P cultures were maintained for a period of 180 days and then used to assess three critical parameters, i.e., expression of virus-encoded proteins, accumulation of viral RNAs, and extracellular infectious virus production. Mock- and acutely infected (3 PFU/cell) naive DF-1 cells collected at 18 h p.i. were used as controls for these assays.

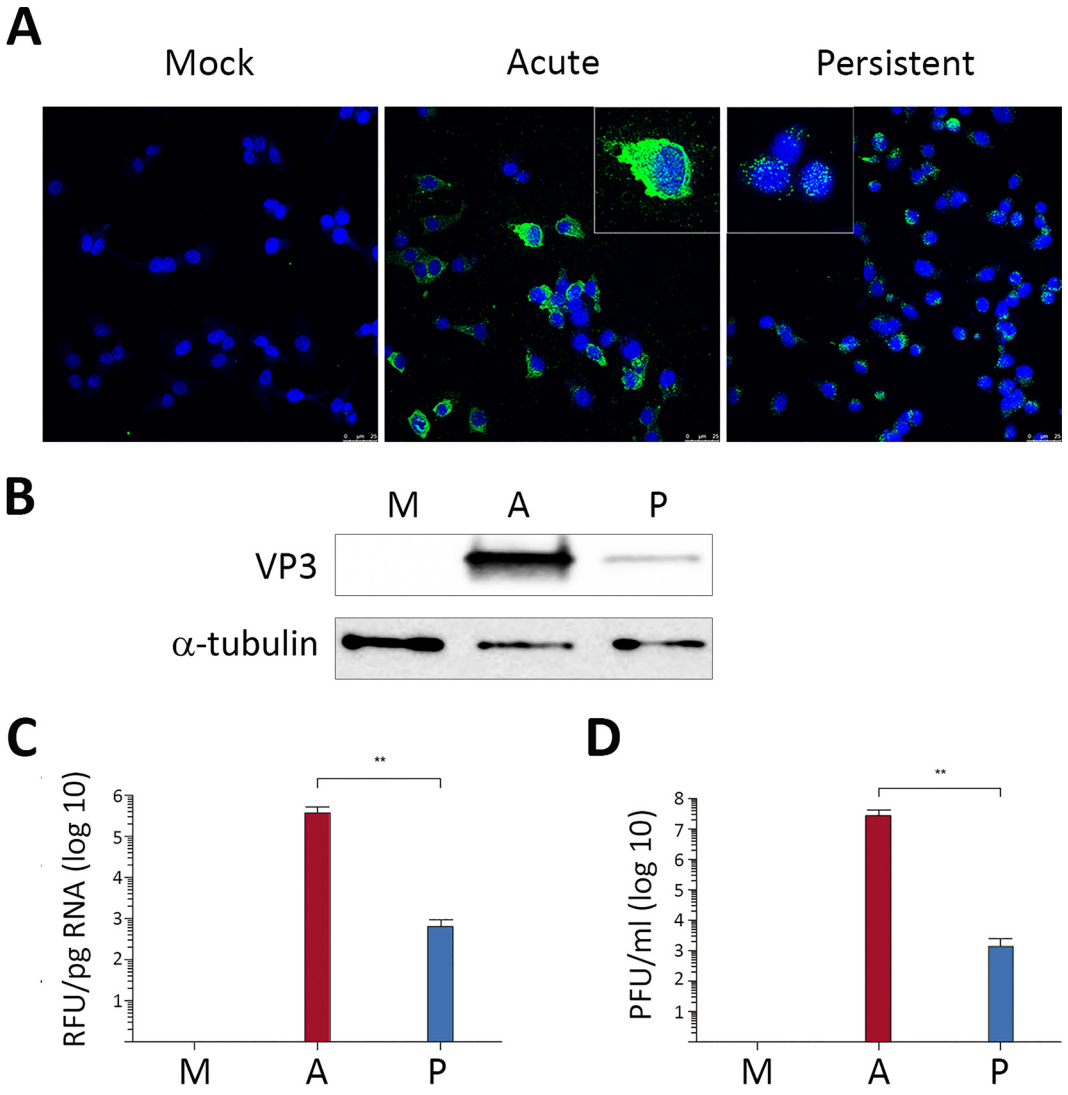

FIG 2 Characterization of persistently infected DF-1P cell cultures. Persistently infected DF-1P cell cultures (P) maintained for 180 days were used to assess the expression of virus-encoded proteins, the accumulation of viral RNAs, and the production of extracellular infectious virus. Mock (M)- and acutely infected (3 PFU/cell) DF-1 cells collected at 18 h p.i. (A) were used as controls for this analysis. (A) Cells were processed for IF microscopy using an antibody specifically recognizing the IBDV structural VP3 polypeptide. Cell nuclei (blue) were stained with DAPI. Insets show higher magnifications (×2.5) of boxed areas. (B) Cell extracts were subjected to SDS-PAGE followed by Western blotting using antibodies specifically recognizing either the IBDV structural VP3 or the cellular α-tubulin polypeptides. (C) RNAs extracted from the different cell cultures were used for RT-qPCR analysis using primers hybridizing at the VP3 coding region (genome segment A). (D) Supernatants collected from the different cell cultures were used for virus titration. Each determination was carried out in triplicate. Presented data correspond to the means ± standard deviations from three independent experiments. Brackets indicate pairwise data comparisons. **, $P < 0.001$ as determined by two-tailed unpaired Student's *t* test.

First, cultures were processed for IF analysis using an anti-VP3 serum. As shown in Fig. 2A, all DF-1P cells showed a positive signal for this polypeptide. It is worth noting that, in contrast to the rather intense cytoplasmic immunostaining detected in acutely infected cells, the VP3 signal found in DF-1P cells was characterized by formation of small perinuclear protein accretions. In line with this observation, Western blotting revealed that the accumulation of the VP3 polypeptide in DF-1P cultures was significantly lower than that detected in acutely infected cells (Fig. 2B). We next compared the relative abundance of the IBDV RNA by reverse transcription and quantitative PCR (RT-qPCR) analysis. As shown in Fig. 2C, accumulation of IBDV RNA in DF-1P cultures was about 1,000-fold lower than that found in acutely infected cells. Similarly,

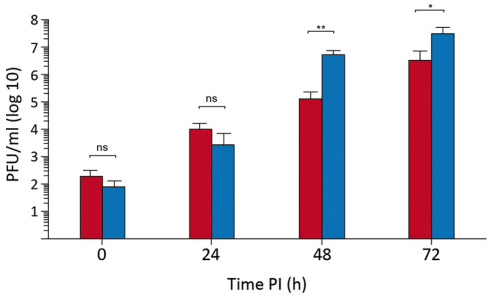

FIG 3 Replication fitness of persistent virus populations. DF-1 cell cultures were infected (0.005 PFU/cell) with supernatants from naive DF-1 cells infected with WT virus (red) or from a 180-day- old DF-1P culture (blue). Infected cell supernatants were collected at the indicated times p.i. and used for virus titration. Each determination was carried out in triplicate. Presented data correspond to the means ± standard deviations from three independent experiments. Brackets indicate pairwise data comparisons. *, $P < 0.01$; **, $P < 0.001$; determined by two-tailed unpaired Student's *t* test. ns, not significant.

extracellular IBDV titers detected in DF-1P cell supernatants were approximately 10,000-fold lower than those found in samples from acutely infected DF-1 cells (Fig. 2D). Results obtained with the three selected DF-1P cultures were nearly identical.

Characterization of viral populations generated during persistent infection. Results described above indicate that both virus replication and infectious virus yields detected in DF-1P cultures are exceedingly lower than those found in acutely infected DF-1 cells, suggesting that persistency entails the selection of viral populations with reduced replication fitness. To analyze this hypothesis, we first determined the nucleotide sequence of the parental (wild-type [WT]) and DF-1P virus populations (P). Comparisons of both genome segments and the three (i.e., VP5, polyprotein, and VP1) virus-encoded polypeptides then were performed (data not shown). Genome differences were minimal, having identity scores of 97.3% and 98% for segments A and B, respectively. Similarly, rather high identity scores were also detected when comparing the proteins encoded by both genomes, i.e., 97.9, 98.2, and 99.5% for VP5, polyprotein, and VP1, respectively.

The growth rates of samples collected from supernatants of naive DF-1 cells infected with WT virus or from DF-1P cells (P) were compared. Owing to the rather low infectious titers found in samples from DF-1P cells, in the range of 10^3 PFU/ml, as shown in Fig. 2, this study was performed by infecting naive DF-1 cell monolayers at a multiplicity of infection (MOI) of 0.005 PFU/cell. As shown in Fig. 3, the replication efficiency of the P virus is slightly greater, rendering extracellular infectious titers about 10-fold higher at 48 and 72 h p.i. than those detected in cells infected with the parental WT virus. Similar results were obtained with P virus populations harvested from the three independent DF-1P cultures.

Next, we sought to determine whether viral populations collected during persistency exhibited an enhanced capacity to establish new persistent infections. For this, a series of experiments were carried out by infecting (0.005 PFU/cell) naive DF-1 cell cultures with either the WT or the P virus. After 4 days, cultures were rinsed, allowed to recover for 3 weeks, and then used to determine the number of surviving clones as described above. No significant differences were found between WT- or P-infected cells, indicating that both virus populations behave similarly regarding the establishment of persistent infections in DF-1 cells (data not shown).

Elimination of infectious IBDV from DF-1P cells. In view of data presented above, it was interesting to compare the behavior of naive DF-1 and DF-1P cells. However, the presence of the persistently infecting IBDV population in DF-1P cells posed a major obstacle for this study. Accordingly, we sought to eliminate the virus using 7-deaza-2′-C-methyladenosine (7DMA), an efficient inhibitor of a wide variety of viral RNA-dependent RNA polymerases, including that encoded by IBDV (14). DF-1P cultures were maintained for 90 days in medium supplemented with 200 μM 7DMA. Thereafter, cultures

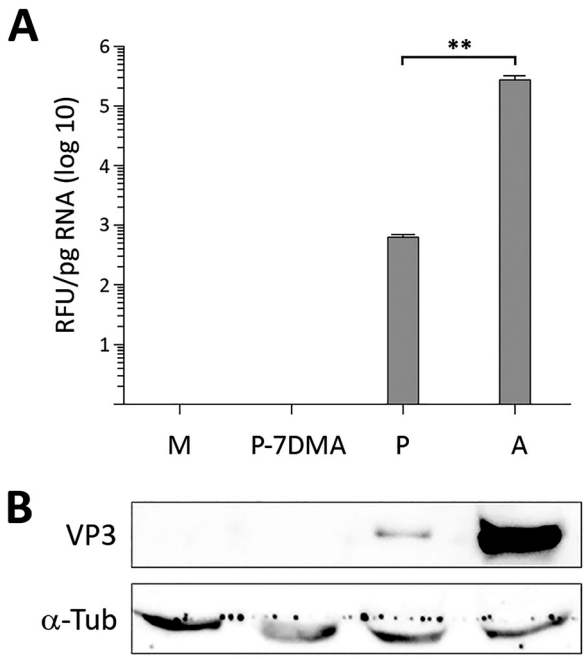

FIG 4 Elimination of infectious IBDV from DF-1P cells. Persistently infected DF-1P cultures were subjected to a prolonged (180-day) treatment with 7DMA, an inhibitor of viral RNA polymerases of RNA viruses. After the treatment, cultures were maintained for 30 days in the absence of the inhibitor to facilitate the recovery of potentially surviving IBDV populations. Thereafter, untreated (P) and 7DMA-treated (P-7DMA) DF-1P cell cultures were used to search for the presence of IBDV RNA and the structural IBDV VP3 polypeptide. Samples from mock [M]- and acutely infected DF-1 (A) cells were used as controls. (A) RNAs extracted from the different cultures were used to perform an RT-qPCR analysis using primers hybridizing at the VP3 coding region (genome segment A). Each determination was carried out in triplicate. Presented data correspond to the means ± standard deviations from three independent experiments. Brackets indicate pairwise data comparisons. **, $P < 0.001$ as determined by two-way analysis of variance (ANOVA). (B) Cell extracts were subjected to SDS-PAGE followed by Western blotting using antibodies specifically recognizing either the IBDV structural VP3 or the cellular α-tubulin polypeptides.

were further maintained for 30 days in normal medium to allow the replication of potentially surviving infectious IBDV.

To assess the effect of the 7DMA treatment, cell extracts were used to perform RT-qPCR and Western blotting to search for the presence of IBDV-specific RNA and the VP3 polypeptide, respectively. Samples from untreated DF-1P and acutely infected (3 PFU/cell) DF-1 cells were used as controls for this analysis. As shown in Fig. 4A and B, the RT-qPCR and Western blot analyses failed to detect either IBDV-encoded RNA or the VP3 polypeptide in cultures subjected to the described 7DMA treatment. Additionally, infectious IBDV was not found in samples from cell supernatants, indicating that the treatment had effectively eliminated IBDV from DF-1P cultures. Cured DF-1P cultures here are termed DF-1PC.

DF-1PC cells exhibit an enhanced susceptibility to establishing persistent IBDV infections. At this point, it was interesting to compare the growth rate of WT IBDV in naive DF-1 and DF-1PC cell cultures. Accordingly, both cell lines were infected with WT IBDV at an MOI of 3 PFU/cell. Cell supernatants were collected at different times (i.e., 24, 48, and 72 h) p.i. and used for virus titration. As shown in Fig. 5A, no significant differences were observed on the extracellular infectious yields generated upon infection of these two cell lines.

Despite the efficient IBDV replication observed with DF-1PC cells, it was readily noticeable that the cell death induced by the infection was much lower in DF-1PC than in the parental DF-1 cell line. To quantitatively assess this initial observation, a kinetic cell death analysis was performed using the 3-(4,5-dimethylthiazol-2-yl)-2,5-diphenyltetrazolium bromide (MTT) assay. DF-1 and DF-1PC cell monolayers were infected with WT IBDV

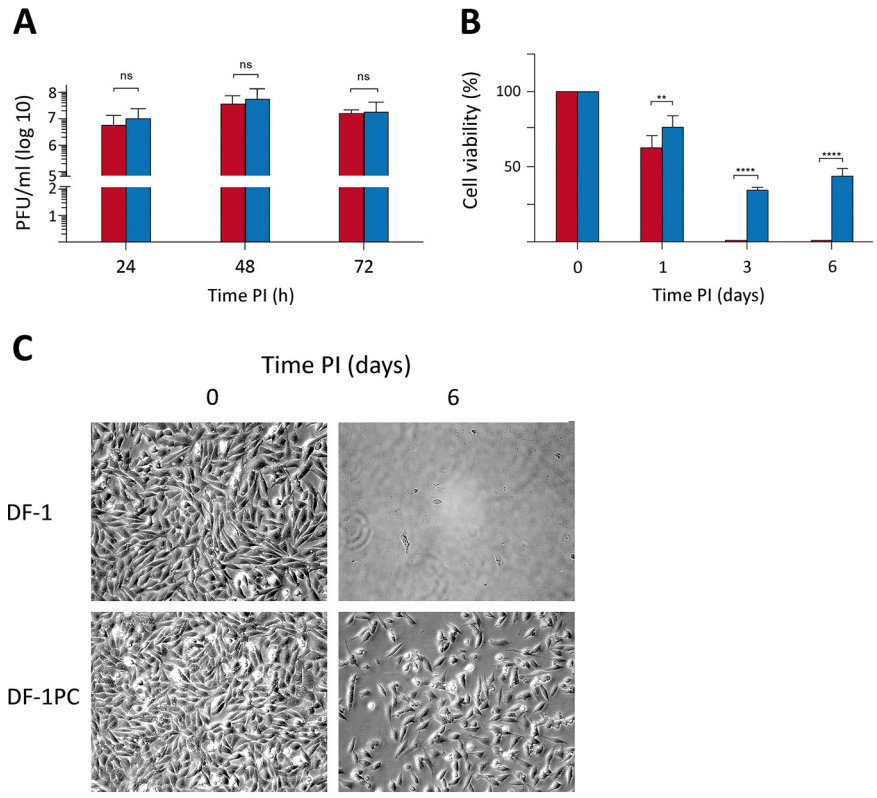

FIG 5 Comparative analysis of naive DF-1 and DF-1PC regarding their susceptibility to IBDV infection and the capacity to survive the acute infection phase. DF-1 (red) and DF-1PC (blue) cell cultures were infected with WT IBDV (3 PFU/cell). (A) Cell supernatants were harvested at the indicated times p.i. and used for virus titration. Presented data correspond to the means ± standard deviations from three independent experiments. Brackets indicate pairwise data comparisons. ns, not significant as determined by two-way ANOVA. (B) Cell viability was determined at the indicated times p.i. using the MTT assay. Presented data correspond to the means ± standard deviations from three independent experiments. Brackets indicate pairwise data comparisons. **, $P < 0.001$; ****, $P < 0.00001$; determined by two-way ANOVA. (C) Phase-contrast microscopy images of infected DF-1 and DF-1PC cell cultures captured at the indicated times postinfection.

(3 PFU/cell), and cell viability determined at 1, 3, and 6 days p.i., respectively. As shown in Fig. 5B, infection of parental DF-1 cells led to a swift reduction of cell viability, reaching undetectable MTT values at 3 days p.i. In contrast, the viability decline of infected DF-1PC cells was significantly less pronounced, reaching its minimal value (ca. 35%) at 3 days p.i. Furthermore, MTT values detected in infected DF-1PC cultures underwent a substantial increase at 6 days p.i., indicating that cells surviving the acute infection phase maintained the capacity to proliferate. Figure 5C shows representative phase-contrast images corresponding to IBDV-infected DF-1 and DF-1PC cultures captured at 1 h and 6 days p.i., respectively, evidencing the existence of a major difference in the capacity of these two cell lines to survive an acute IBDV infection phase. Notably, infected DF-1PC cultures reestablished fully confluent, persistently infected monolayers 8 to 10 days after the initiation of the infection.

The JAK-STAT signaling pathway is functionally blocked in DF-1PC cells. We have recently shown that type I IFN plays a crucial role in the fate of IBDV-infected cells (14). Thus, while pretreatment of cells with IFN-α induces a solid protection against IBDV replication, its addition early after infection leads to a massive apoptotic response that wipes out infected cell cultures (14).

Therefore, it was important to compare the capacity of DF-1 and DF-1PC cells to respond to type I IFN. To this end, DF-1 and DF-1PC cultures were left untreated or were treated with IFN-α (1,000 IU/ml) for 16 h. Thereafter, cultures were incubated with

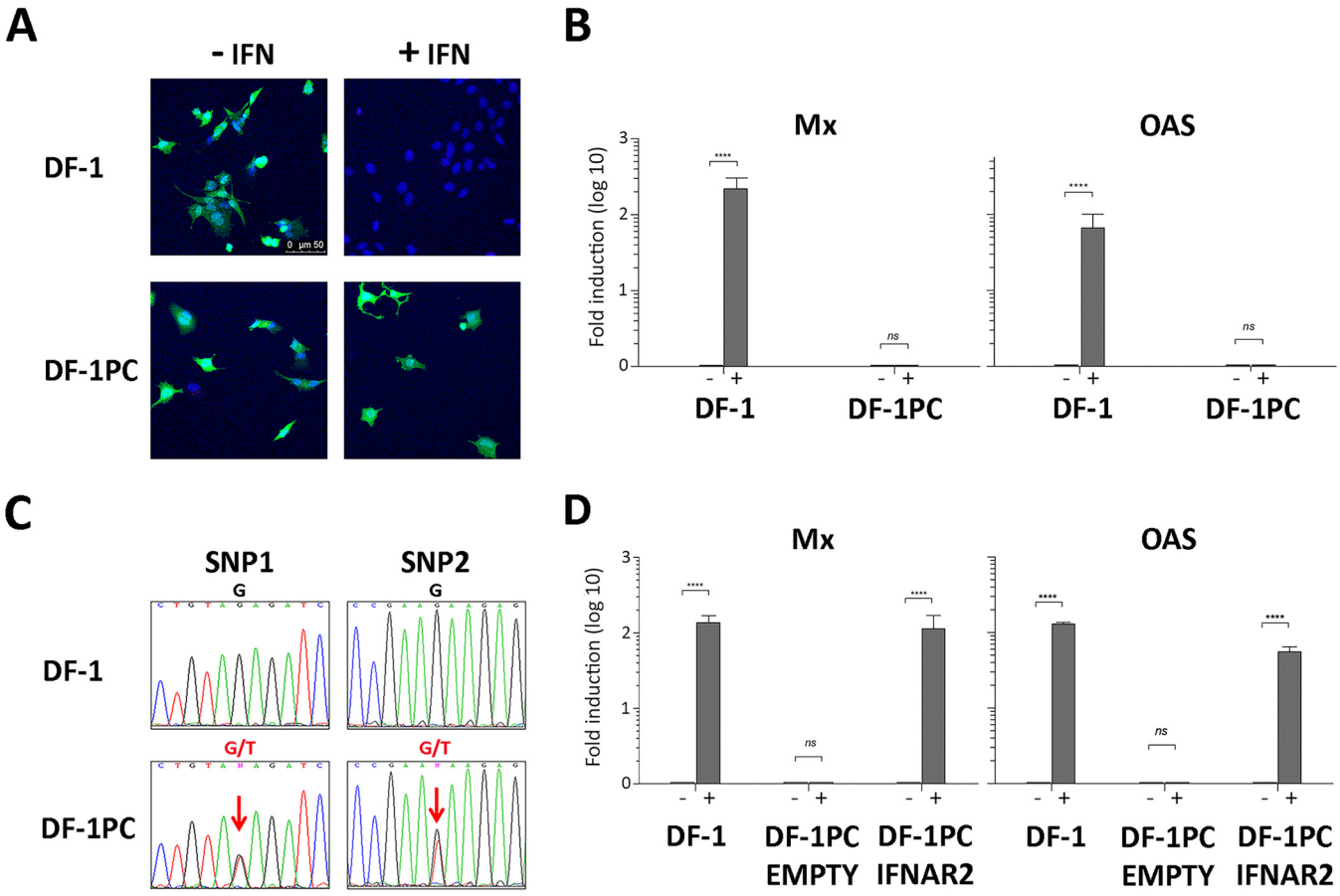

FIG 6 Capacity of naive DF-1 and DF-1PC cells to respond to chicken IFN-α. (A and B) DF-1 and DF-1PC cell cultures were treated with IFN-α (1,000 IU/ml) (+IFN) or left untreated (−IFN) for 16 h. Cultures were then used to assess their susceptibility to VSV infection or the expression of the Mx and OAS ISGs. (A) Cultures were infected (1 PFU/cell) with VSV-GFP expressing the GFP polypeptide. At 12 h p.i., cultures were incubated with DAPI to stain cell nuclei and then observed under fluorescence microscopy. (B) Cultures were harvested and subjected to RNA extraction. Mx and OAS expression levels were determined by RT-qPCR. Presented data correspond to the means ± standard deviations from three independent experiments. Brackets indicate pairwise data comparisons. ****, $P < 0.00001$ as determined by two-way ANOVA. ns, not significant. (C) Detection of single-nucleotide polymorphisms in IFNAR exon 10. Genomic DNA isolated from DF-1 and DF-1PC cell cultures was subjected to PCR using oligonucleotides OL_IFNAR2.1 and OL_IFNAR2.2. The resulting amplicons, spanning the region of interest of IFNAR2 exon 10, were subjected to conventional Sanger sequencing using the same oligonucleotides. Panels show sequencing chromatogram regions of interest (holding DF-1PC SNPs) from DF-1 and DF-1PC amplicons, respectively. Lettering above chromatograms corresponds to detected nucleotides, namely, A (green), C (blue), G (black), and T (red). Sequence ambiguities (G/T) are indicated as N (magenta). (D) DF-1PC cells were transfected with pCI-neo/chIFNAR2-FLAG, a mammalian expression vector expressing a full-length version of the chicken IFNAR2 gene (DF-1PC IFNAR2). Control DF-1PC cultures were transfected with the pCI-neo parental vector (DF-1PC Empty). At 24 h posttransfection, cultures were treated with 1,000 IU of IFN-α (+) or left untreated (−) for 16 h. IFN-treated and untreated DF-1 cell cultures were used as additional controls for these experiments. RNA isolated from the different cell cultures was used to assess the transcriptional activation of the Mx and OAS genes by RT-qPCR. Presented data correspond to the means ± standard deviations from three independent experiments. Brackets indicate pairwise data comparisons. ****, $P < 0.00001$ as determined by two-way ANOVA. ns, not significant.

a recombinant vesicular stomatitis virus expressing the green fluorescent protein (VSV-GFP) (1 PFU/cell). VSV is extremely sensitive to the antiviral response induced by type I IFNs, providing a simple assay to assess IFN responsiveness. At 12 h p.i., cultures were incubated with DAPI to stain cell nuclei and then visualized using fluorescence microscopy to detect GFP expression (Fig. 6A). As expected, untreated DF-1 cells showed an intense GFP signal, indicating that they were efficiently infected with VSV-GFP. In contrast, IFN-α-treated DF-1 cells were fully protected, as evidenced by the absence of a fluorescent GFP signal. Interestingly, both untreated and IFN-α-treated DF-1PC showed an intense green fluorescence revealing the VSV-GPF infection, indicating the incapacity of this cell line to respond to IFN-α.

To further verify this finding, an alternative approach was used. DF-1 and DF-1PC monolayers were left untreated or were treated with IFN-α (1,000 IU/ml) for 16 h and then used to extract cellular RNA. These RNA samples were used to perform RT-qPCR

analyses to check the transcriptional activation of two interferon-stimulated genes (ISG), i.e., Mx and 2′,5′-oligoadenylate synthetase (OAS), generally used as activation markers of the Janus kinase-signal transducer and activator of transcription protein (JAK-STAT) signaling pathway (15). As shown in Fig. 6B, DF-1 cells efficiently responded to the IFN-α treatment, triggering a strong transcriptional activation of both Mx and OAS genes. In contrast, basal Mx and OAS RNA levels were detected in both treated and untreated DF-1PC cells. These results further confirmed the incapacity of the DF-1PC cell line to respond to IFN-α.

Genetic analysis of DF-1 and DF-1PC cells. The avian JAK-STAT signaling pathway is relatively simple, encompassing a reduced number of protein components (reviewed in reference 16). Despite this apparent simplicity, there are many potential mutations capable of impairing the pathway's functionality. In view of this, high-throughput next-generation sequencing (NGS) was used to perform a whole sequencing analysis of the DF-1 and DF-1PC cell genomes as described in Materials and Methods.

Assembled DF-1 and DF-1PC genomes were annealed to the *Gallus gallus* (red junglefowl breed isolate RJF number 256 [GenBank accession number GRCg6a]) genome. Both assembled genomes cover over 98% of the reference genome with an average sequencing depth of 35× (data not shown). Next, DF-1 and DF-1PC exomes were compared to the reference chicken exome to detect differential single-nucleotide polymorphisms (SNPs), insertions, and deletions. Differential insertions or deletions at the DF-1 and DF-PC exomes were not found. However, the analysis led to the detection of two SNPs exclusively found within the DF-1PC exome. Both SNPs consisted of a thymidine (T)-to-guanine (G) substitution at nucleotide positions 106,590,841 (SNP1) and 106,591,114 (SNP2), respectively. SNP1 and -2 were found within 57% and 46%, respectively, of DF-1PC sequencing reads spanning the described nucleotides.

Both DF-1PC-specific mutations map at chromosome 1 (NCBI reference sequence NC_006088.05) within the last exon (exon 10) of the gene encoding the IFN-α/β receptor subunit 2 (IFNAR2) (GenBank accession number AF082665.1) (17).

To confirm NGS sequencing data, amplicons spanning the IFNAR2 exon 10 region holding both mutations were generated by PCR using genomic DNA isolated either from DF-1 or DF-1PC cells as templates. Oligonucleotides OL_IFNAR2.1 (5′-CCATCCC ATCAGCCTGGAAAT) and OL_IFNAR2.2 (5′-TGCACATTGCCAGTCAACAG), hybridizing at nucleotide positions 660 to 688 and 1349 to 1368, respectively, of the IFNAR2 DNA were used as PCR primers. DF-1- and DF-1PC-derived amplicons were subjected to conventional nucleotide sequencing analysis using oligonucleotides OL_IFNAR2.1 and OL_IFNAR2.2. As shown in Fig. 6C, the presence of double nucleotide (G/T) signals at SNP1 and -2 positions in chromatograms from DF-1PC amplicons fully confirmed NGS data. As expected, amplicons derived from DF-1 genomic DNA presented single (G)-nucleotide signals at equivalent positions.

At this point, it was important to determine whether the detected mutations were homo- or heterozygous. To answer this question, the DF-1PC amplicon was cloned into the pGEM-T Easy plasmid vector. Thereafter, recombinant plasmids purified from 20 independent ampicillin-resistant *Escherichia coli* colonies were purified and used for nucleotide sequencing using the above-described primers. All analyzed plasmids contained single mutations, 9 of them harboring SNP1 and the remaining 11 SNP2. These results indicate that mutations are heterozygous, with each DF-1PC IFNAR2 allele containing a single G/T substitution at different exon 10 positions.

The three persistently infected DF-1P cell lines were shown to harbor the same mutations, indicating that both mutations were already present before the 7DMA treatment.

DF-1PC cells encode C-terminally truncated IFNAR2 polypeptides. The chicken IFNAR2 gene encodes the IFNAR2 protein precursor, a polypeptide (508 residues) encompassing a signal peptide that is removed during its transport to the cell membrane. Mature IFNAR2 is a type I transmembrane polypeptide including an N-terminal ectodomain (216 residues), a transmembrane region (20 residues), and a cytoplasmic domain (246 residues). The ectodomain is responsible for the interaction of the protein

with its cognate cytokine ligands and the subsequent assembly of ternary receptor complexes with IFNAR1. IFNAR1 and IFNAR2 cytoplasmic domains are accountable for the propagation of the activation signal to effector proteins, i.e., JAK, STAT1, and TYK2 (reviewed in reference 18).

The G-to-T nucleotide substitutions found in IFNAR2 of DF-1P and DF-1PC cells transform GAT and GAA codons, encoding two glutamic acid (E) residues, i.e., E301 and E392, into TAG and TAA translation termination codons, respectively. Indeed, these mutant IFNAR2 genes encode C-terminal truncated IFNAR2 polypeptides lacking either 107 or 208 residues, respectively. Unfortunately, the lack of specific antibodies recognizing the chicken IFNAR2 polypeptide prevented visualization of the truncated proteins.

The ablation of the IFNAR2 cytoplasmic domain, essential for the transduction of the JAK-STAT activation signal (19), would explain the incapacity of DF-1PC cells to respond to type I IFN. To confirm this prediction, we sought to determine whether the ectopic expression of a full-length version of the IFNAR2 polypeptide rescues IFN-α responsiveness. Hence, a recombinant version of the chicken IFNAR2 gene was synthesized and cloned into the expression vector pCI-neo, generating the pCI-neo/chIFNAR2-Flag plasmid. DF-1PC cells were transfected either with empty pCI-neo or pCI-neo/chIFNAR2-FLAG. At 24 h posttransfection, cultures were left untreated or treated with 1,000 IU of IFN-α for 16 h and then used for RNA extraction. RNA samples were used to assess Mx and OAS transcription by RT-qPCR. RNAs from treated and untreated DF-1 cell cultures were used as controls. As shown in Fig. 6D, while pCI-neo-transfected DF-1PC cultures did not respond to the treatment, those transfected with pCI-neo/chIFNAR2-FLAG readily reacted to IFN-α, triggering a ca. 100-fold increase in the expression of both ISGs. These results indicate that the ectopic expression of the full-length recombinant IFNAR2-Flag protein restores the functionality of the JAK-STAT pathway in DF-1PC cells. Additionally, these results ruled out the existence of potentially undetected genetic alterations also affecting the functionality of this pathway.

In view of these results, we decided to analyze the responsiveness to IFN-α of cells that remain alive from an acute IBDV infection. For this, cell islets generated after a 21-day recovery period following the acute IBDV infection were treated with 1,000 IU of IFN-α for 16 h and then challenged with VSV-GFP as described above. Nearly 60% of the islets were protected against VSV infection, indicating they are still responsive to IFN (data not shown). Taken together, our results suggest that the early surviving IFN-responsive persistently infected cells keep dying over time during continuous cell passaging, and that only cells defective in the JAK-STAT pathway subsist indefinitely.

Effect of the impairment of the JAK-STAT pathway on the establishment of IBDV persistent infections on human HeLa cells. We have shown that the inactivation of the JAK-STAT pathway significantly lessens IBDV-induced cell death in avian DF-1 cells and enhances their susceptibility to initiate persistent infections. It was important to ascertain whether or not this is a general trait also operating in other IBDV-susceptible cells. Concerning this, Urin et al. (20) have recently described the generation of a set of human HeLa knockout (KO) cell lines selectively lacking every gene participating in the JAK-STAT pathway. We borrowed the HeLa IFNAR2 KO line, unable to respond to type I IFN, to analyze the effect that the functional inactivation of the JAK-STAT pathway may have on the fate of IBDV-infected HeLa cells.

We first compared the death rate of parental (WT) and IFNAR2 KO cells induced by the IBDV infection using the MTT cell viability assay. Cell monolayers were infected (3 PFU/cell), and cell viability was determined at 1, 3, and 6 days p.i. As shown in Fig. 7A, the behavior of both cell lines was strikingly different. WT cells were swiftly killed by the infection, reaching viability values nearing 0% at 6 days p.i. In contrast, the viability of infected IFNAR2 KO HeLa cells remained largely unaltered at the beginning of the infection (1 to 3 days p.i.) and grew at later times, reflecting the capacity of infected cells to proliferate. In line with this observation, infected IFNAR2 KO cells readily became persistently infected. As is the case with DF-1P cells, persistently infected IFNAR2 KO HeLa cells also showed a reduced accumulation of the IBDV VP3 polypeptide compared to acutely infected cells (Fig. 7B).

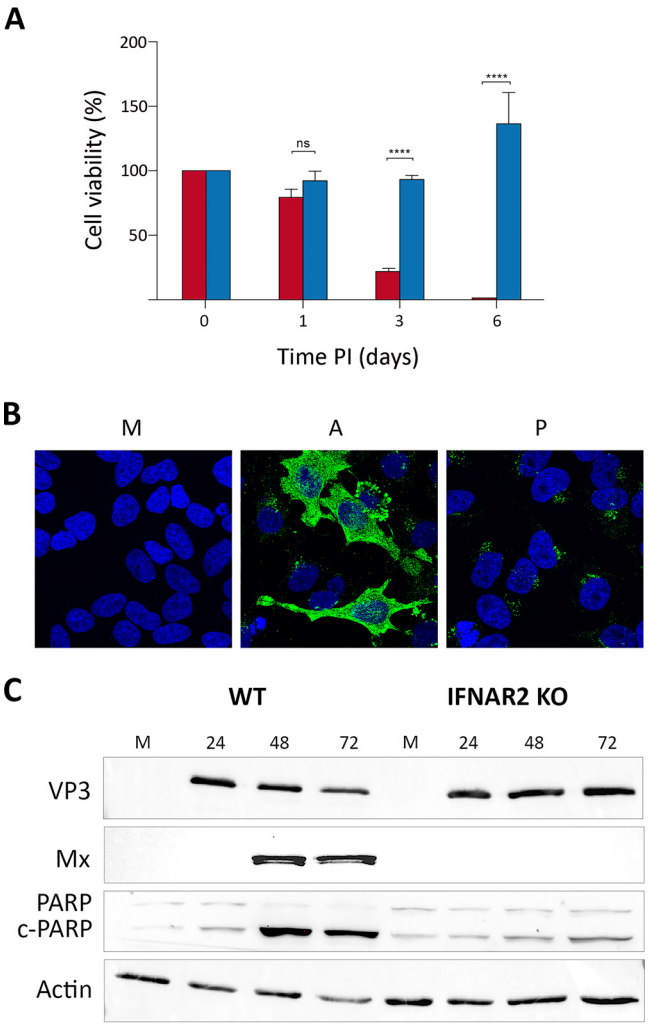

FIG 7 Effect of the inactivation of the JAK-STAT pathway on the fate of IBDV-infected HeLa cells. (A) WT (red) and IFNAR2 KO HeLa (blue) cell cultures were infected with WT IBDV (3 PFU/cell). Cell viability was determined at the indicated times p.i. using the MTT assay. MTT values recorded immediately after infection were considered 100% cell viability. Presented data correspond to the means ± standard deviations from three independent experiments. Brackets indicate pairwise data comparisons. ****, $P < 0.00001$ as determined by two-way ANOVA. ns, not significant. (B) Persistently infected IFNAR2 KO cells (P) maintained for 2 months were processed for IF analysis using an antibody specifically recognizing the IBDV structural VP3 polypeptide. Cell nuclei (blue) were stained with DAPI. Mock-infected (M) and acutely infected (3 PFU/cell, fixed at 48 h p.i.) (A) cells were used as controls. (C) Infected (3 PFU/cell) WT and IFNAR2 KO cell cultures were collected at the indicated times p.i. Mock-infected (M) cell cultures were used as controls. The corresponding extracts were subjected to SDS-PAGE followed by Western blotting using antibodies against the virus-encoded VP3 and the cellular Mx, PARP, and actin proteins. The PARP cleavage product is denoted c-PARP.

To further assess the differential behavior of WT and IFNAR2 KO HeLa cells, Western blotting was performed using cell extracts collected at different times p.i. (i.e., 24, 48, and 72 h). Samples from mock-infected cells were used as controls. As shown in Fig. 7C, both WT and IFNAR2 KO HeLa cells were readily infected with IBDV, showing similar VP3 accumulation levels at 24 h p.i. As expected, while infection of WT cells efficiently triggered robust Mx protein expression, infected IFNAR2 KO cell extracts were void of this protein, confirming their incapacity to activate the type I IFN-mediated gene expression in response to IBDV infection. The proteolytic cleavage of poly(ADP-ribose) polymerase (PARP) is generally used as an early apoptotic marker (21). Accordingly, we monitored PARP cleavage to compare the apoptotic response of infected WT and IFNAR2 KO cells. As expected, infection of WT cells resulted in a conspicuous PARP

cleavage, detectable from 24 h p.i. onwards. In contrast, this effect was significantly abridged in IFNAR2 KO cells, showing a rather modest increase of the cleaved PARP (c-PARP) product at 72 h p.i. Consistent with the observed apoptotic induction observed in WT HeLa cells, the amount of both VP3 and the cellular actin polypeptide, used as a protein loading control in this experiment, was significantly reduced in WT-infected cells collected at 72 h p.i.

Taken together, these results show that, similar to what had been found in DF-1 cells, the obliteration of the JAK-STAT signaling pathway significantly enhances the capacity of HeLa cells to survive the acute infection phase and facilitates the establishment of IBDV persistent infections.

DISCUSSION

Although infection of DF-1 cells with IBDV results in massive cell death, a minor, yet consistent, cell fraction endures the acute infection phase, giving rise to a collection of persistently infected cell clones, holding from 10 to several thousand cells at 21 days p.i. This initial size variation suggests the existence of major differences in the capacity of surviving cells to withstand IBDV replication. Our results indicate that continuous cell passaging progressively narrows down the initial heterogeneity. Hence, although persistently infected cultures described here were not subjected to cell cloning, genome sequencing data showed that the three DF-1P lines characterized during our study share identical mutations on the IFNAR2 gene, suggesting that they originated from a preexisting DF-1 cell subset already holding these mutations.

It seems reasonable to hypothesize that the long-term passaging of persistently infected cultures enables a Darwinian process resulting in the selection of clonal cell populations harboring the fittest genotype to sustain proliferation while enduring a significantly lessened, yet productive, IBDV replication. Indeed, the repeated selection of persistently infected cell clones incapable of responding to type I IFN described here underscores the crucial role of the innate antiviral cell response and, in particular, that of the JAK-STAT pathway on the fate of IBDV-infected cells.

Virus replication taming, an IBDV persistency hallmark. As evidenced in different virus-cell systems, persistent viral infections require the successful interplay of cellular and viral mechanisms capable of sustaining a precise equilibrium between virus replication and cell proliferation. The modulation of virus replication is a common finding in persistent infections, likely being a requirement for the initiation of persistency (22).

A comparison of elemental virus replication parameters (i.e., virus yield and genome and protein accumulation) performed in acute and persistent IBDV infections indicates that persistency entails a major downregulation of virus replication. IBDV downregulation could have been associated with the selection during the initial stages of the persistency of a virus population(s) exhibiting reduced replication fitness. However, contrary to this simple notion, viruses harvested from persistently infected DF-1 cells showed an enhanced replication capacity compared to the WT parental virus. A similar situation was found during the characterization of BHK-21 cells persistently infected with foot-and-mouth disease virus (FMDV; *Picornaviridae*), where it was shown that FMDV became progressively more virulent upon serial passages of persistently infected cells (23). In both cases, IBDV and FMDV, persistency results in the selection of virus populations exhibiting enhanced fitness. Nonetheless, we cannot rule out that the higher titers detected in cells infected with the virus from persistently infected cells might be due to higher viability of these cells compared with those infected with the WT virus.

Although the possible implication of other genetic elements, e.g., microRNAs (24), cannot be ruled out at this point, data gathered from a wide variety of viruses, including birnaviruses, suggest that the downregulation of IBDV replication is related to the presence of defective virus genomes (DVGs). These aberrant genomes, arising from errors during the replication of many viruses, retain the replication capacity of standard

viral genomes. It has been extensively documented that DVGs interfere with the replication of parental viruses, thereby contributing to the establishment of persistent infections both *ex* and *in vivo* (25, 26).

The role of the JAK-STAT pathway. The type I IFN-dependent antiviral response entails two interrelated signaling cascades known as transactivation and JAK-STAT pathways. The transactivation pathway, involving a large number of sentinel and effector proteins, is activated by the presence of pathogen-associated molecular patterns (e.g., nucleic acids, proteins, or lipids) at different cell compartments, triggering the expression of type I IFNs as well as an ISG subset, including IFN response factors, pattern recognition receptors, and some antiviral effectors (16). Although, for the sake of concision, data concerning the transactivation capacity of DF1-PC and HeLa are not presented in this report, we have documented that this pathway remains fully functional in both DF-1PC and HeLa IFNAR2 KO cell lines.

Upon their release from infected cells, IFNs interact with both uninfected and infected cells. This interaction activates the JAK-STAT pathway, triggering the expression of the whole ISG set and the concomitant implementation of the antiviral defense program in uninfected bystander cells. However, it has also been well documented that the concurrent activation of both type I IFN pathways induces a vigorous apoptotic response that eliminates virus-infected cells (reviewed in reference 27). Indeed, the comparative analysis performed with DF-1 and DF-1PC cells indicates that the functional inactivation of the JAK-STAT pathway significantly reduces the apoptotic response induced by the infection, strongly affecting IBDV-induced death rates. Thus, while MTT cell viability values recorded in WT-infected DF-1 cells become negligible at 72 h p.i., approximately 30% of infected DF-1PC cells remain alive at this time. A comparison of data corresponding to the recovery of persistently infected cell clones generated upon infection of naive DF-1 cells, 0.023% of the total infected population, with 30% cell survival recorded in infected DF-1PC populations, indicates that the inactivation of the JAK-STAT pathway enhances over 1,000-fold the capacity of DF-1 cells to survive the acute IBDV infection phase.

Results obtained with WT and IFNAR2 KO HeLa cells nicely recapitulate the differential behavior detected in infected DF-1 and DF-1PC cells, showing again that the inactivation of the JAK-STAT pathway affords a striking increase of the capacity of infected cells to survive the acute infection phase and to initiate persistent infections. In line with previous reports, results presented here show that the death of IBDV-infected cells is directly related to the apoptotic response triggered by the infection, and that this is largely owed to the activity of type I IFNs. Indeed, a major conclusion of our study is that type I IFNs act as a major barrier preventing the establishment of IBDV persistent infections.

As stated above, IBDV replication in HeLa cells is significantly slower than that in DF-1 cells. A major difference is also evident in the production of infectious virus yields, being significantly higher (15- to 20-fold) in DF-1 cells. Interestingly, despite the fact that both cell lines, DF1-PC and HeLa IFNAR2 KO, share the inability to respond to type I IFN, the efficiency with which HeLa IFNAR2 KO cells develop persistent infections is significantly higher than that observed in DF-1PC cells. This observation suggests the existence of an inverse correlation between replication efficiency and the proneness to establishing persistent infections.

Although IgM-bearing chicken bursal lymphocytes are the main IBDV cell target, it has been shown that, with a much lower efficiency, the virus also replicates in cells of the monocyte-macrophage lineage (28). It is tempting to speculate that this cell lineage plays a role in the establishment of *in vivo* persistent infections, as was previously suggested (9, 28, 29).

Additional factors contributing to the apoptotic response in IBDV-infected cells. Our data indicate that the functional disruption of the JAK-STAT pathway does not completely preclude IBDV-mediated apoptosis, suggesting that another factor(s) associated with IBDV replication processes also contributes to this phenomenon.

It can be envisaged that the hefty accumulation of both virus double-stranded RNA and proteins and the assembly of huge cytoplasmic arrays holding thousands of

closely packed virions, along with the appropriation of the biosynthetic machinery during the acute IBDV infection phase, can significantly alter cellular homeostasis, affording additional proapoptotic stimuli. Regarding this, the availability of IFN-α/β-unresponsive DF-1PC and HeLa IFNAR2 KO cells might help in the identification of other factors, viral and/or cellular, contributing to the obliteration of IBDV-infected cells. Indeed, both cell lines provide a powerful tool to further dissect the molecular bases of the IBDV-induced cellular pathogenesis.

Concluding remarks. As recently evidenced with Ebola virus (EBOV), persistently infected asymptomatic individuals support the long-term maintenance and resurgence of EBOV epidemics in apparently virus-free geographical areas (30). Regarding IBDV, the relentless reemergence of virus outbreaks, even in areas under intense vaccination programs and strict hygienic measures, suggests the existence of undetected virus reservoirs. Indeed, persistently infected birds might play an important role in IBDV epidemiology. Hopefully, data presented here might help in stimulating interest in this largely overlooked phenomenon.

MATERIALS AND METHODS

Cells, viruses, and infections. DF-1 (chicken embryonic fibroblasts, ATCC number CRL-12203) and HeLa (human epithelial cervical cancer cells) were grown in Dulbecco's modified Eagle's medium (DMEM) supplemented with penicillin (100 U/ml), streptomycin (100 mg/ml), and 5% fetal calf serum (FCS) (Sigma). IBDV infections were performed on preconfluent (ca. 75%) cell monolayers with the Soroa strain, a cell-adapted serotype I virus, diluted in DMEM at an MOI of 3 PFU per cell, unless otherwise stated. After adsorption (1 h, 37°C), the medium was replaced with fresh DMEM supplemented with 2% FCS. Infected cultures were maintained at 37°C. Infections with the recombinant stomatitis vesicular stomatitis virus expressing the GFP protein (VSV-GFP) (31) were performed in the same way.

Virus titrations. For IBDV titrations, supernatants from cultures infected with IBDV were collected and subjected to centrifugation (5,000 $\times$ *g* for 5 min) at 4°C to remove cell debris. Clarified cell supernatants were used to determine extracellular virus titers by plaque assay using semisolid agar overlays followed by immunostaining as previously described (32).

IFN-α. The recombinant chicken IFN-α used in our experiments was expressed, purified, and titrated in our laboratory as previously described (14).

Light microscopy. Cell cultures grown onto glass coverslips were washed with PBS, fixed with 4% paraformaldehyde (Sigma) for 30 min, and then extensively rinsed with PBS. Cells were permeabilized by incubation with PBS containing 0.5% Triton X-100 (Sigma) for 5 min. Coverslips were blocked for 20 min using a solution of PBS containing 5% FCS and then incubated with a rabbit anti-VP3 serum (33) for 18 h at 4°C. Thereafter, coverslips were repeatedly washed in PBS and incubated with goat anti-rabbit IgG coupled to Alexa-488 diluted in PBS supplemented with 1% FCS for 45 min at 20°C. Cell nuclei were stained with 2-(4-amidinophenyl)-6-indolecarbamidine dihydrochloride (DAPI; Sigma) diluted in PBS for 30 min at 20°C. Finally, coverslips were dehydrated with ethanol and mounted with ProLong antifade reagent (Invitrogen). Cells infected with VSV-GFP were washed with PBS and fixed with 4% paraformaldehyde (Sigma) for 30 min, and after an extensive wash with PBS, cell nuclei were stained as described above. Samples were visualized by epifluorescence using a Leica TCS-Sp5 microscope confocal system. Fluorescent signals detected by confocal laser scanning microscopy were recorded separately by using appropriate filters. Images were captured using the LASAF v.2.6.0 software package (Leica Microsystems).

Western blotting. Samples used for Western blot analyses were prepared by removing media from cell monolayers and then suspending cells in ice-chilled disruption buffer (0.5% Triton X-100, 50 mM KCl, 50 mM NaCl, 20 mM Tris-HCl [pH 7.5], 1 mM EDTA, 10% glycerol, complete protease inhibitor cocktail [Roche]). Samples were mixed (vol/vol) with 2$\times$ Laemmli's sample buffer and heated at 95°C for 5 min before electrophoresis. Electrophoreses were performed on 12% polyacrylamide gels. Gels were subjected to electroblotting onto Hybond-C nitrocellulose membranes. Membranes were blocked with 5% nonfat dry milk in PBS for 1 h at room temperature and then incubated for 18 h at 5°C with the appropriate antisera. Thereafter, membranes were extensively washed with PBS and incubated with the corresponding secondary antibodies coupled to horseradish peroxidase (HRP). Immunoreactive bands were detected by chemiluminescence (Amersham ECL Prime Western Blotting Detection Reagent). Antibodies used in our experiments are listed in Table 1.

RT-qPCR analysis. Total RNA was isolated by using the Macherey-Nagel NucleoSpin RNA plus XS kit (ThermoFisher Scientific) according to the manufacturer's instructions. Purified RNAs (300 to 500 ng) were reverse transcribed into cDNA by using SuperScript III (Invitrogen) reverse transcriptase and random primers. The resulting cDNA samples were subjected to qPCR using the gene-specific primers listed in Table 2. Reactions were performed in triplicate by using Power SYBR green PCR master mix (ThermoFisher Scientific) according to the manufacturer's protocol and by using an Applied Biosystems 7500 real-time PCR system instrument. Reactions were performed with steps of 2 min at 50°C; 10 min at 95°C; 40 cycles of 15 s at 95°C and 1 min at 60°C; and finally, 15 s at 95°C, 1 min at 60°C, 30 s at 95°C, and 15 s at 60°C to build the melt curve. Gene expression levels were normalized to the glyceraldehyde-3-phosphate dehydrogenase (GAPDH) gene, and the results were calculated as fold

TABLE 1 List of antibodies used for Western blotting

Protein	Source	Designation
Actin	Santa Cruz Biotechnology	sc-47778
Tubulin	Cell Signaling	2125
PARP	Cell Signaling	9542S
Mx	Abcam	ab95926
Mouse IgG HRP conjugate	Merck	A4416
Rabbit IgG HRP conjugate	Merck	A0545

changes in gene expression relative to mock-infected cells by using the delta-delta C_T (threshold cycle) method of analysis.

Cell viability assays. Cell viability was determined using the MTT assay kit (Abcam), based on the conversion of water-soluble 3-(4,5-dimethylthiazol-2-yl)-2,5-diphenyltetrazolium bromide (MTT) to an insoluble formazan product, by following the manufacturer's instructions. Cell monolayers were incubated for 3 h with DMEM supplemented with the MTT reagent. After this period, cell medium was replaced by plain DMEM and further incubated for 30 min. Thereafter, media were replaced by dimethyl sulfoxide (DMSO) and maintained for 15 min. All incubations were carried out in the dark under normal culture conditions (37°C, 5% CO_2). Finally, samples were harvested and used to determine the absorbance (Abs) at 570 nm. The percentage of viable cells was determined using the following equation: % viable cells = $(Abs_{sample} - Abs_{blank}/Abs_{control} - Abs_{blank}) \times 100$. Controls correspond to cell cultures collected at the beginning of the experiment. Blank corresponds to empty culture wells.

IBDV genome sequencing. Complete genome sequencing of viruses was performed as previously described (34), with minor modifications. Briefly, viral RNA was extracted from either DF-1 cultures infected with the WT virus or DF-1P cells using the QIAamp viral RNA minikit (Qiagen) according to the manufacturer's instructions. Each segment genome segment was RT-PCR amplified in two fragments using previously described primers (34). Full-length sequencing of each segment was performed in both directions on three independently produced PCR products.

High-throughput cell genome analysis. Genomic DNA was isolated from DF-1 and DF-1PC cell cultures using the Wizard genomic DNA purification kit by following the manufacturer's instructions. A total amount of 1.5 μg DNA per sample was used as the input material for the DNA sample preparations. Sequencing libraries were generated using a TruSeq library construction kit (Illumina) by following the manufacturer's recommendations, and index codes were added to attribute sequences to each sample. Briefly, the DNA samples were fragmented by sonication to a size of 350 bp, end polished, A tailed, and ligated with the full-length adaptor for Illumina sequencing with further PCR amplification. After the library was constructed, a preliminary quantification was performed using Qubit 2.0 (ThermoFisher Scientific), and the library concentration was diluted to 1 ng/μl. The libraries then were analyzed for size distribution using an Agilent2100 Bioanalyzer and quantified using real-time PCR. After the library was qualified, library preparations were sequenced on an Illumina HiSeq platform and paired-end reads were generated. The original data obtained from the high-throughput sequencing were transformed to sequenced reads by base calling. Raw data were recorded in a FASTQ file containing sequenced reads and corresponding sequencing quality information. The sequenced reads were filtered to remove low-quality reads and adapters. After this process, clean reads were mapped to the reference genome for subsequent variation analysis. The bwa software (35) was used for the comparison of short reads obtained from high-throughput sequencing to the *Gallus gallus* (red junglefowl breed isolate RJF number 256 [GenBank accession number GRCg6a]) genome. The position of clean reads on the reference genome was determined by alignment, and the information, such as the depth of sequencing of the samples and the genome coverage, were counted and used for variation detection. Individual SNPs and insertions-deletions (InDels) were detected using SAMTOOLS (36) and annotated using the ANNOVAR software (37). Library construction, high-throughput sequencing, sequence alignments, and SNP and InDel detection and annotations were performed by CD Genomics (NY, USA).

PCR cloning and sequencing. Genomic DNA fragments generated by PCR were cloned into the pGEM-T Easy plasmid vector using the pGEM-T Easy vector system (Promega) by following the manufacturer's instructions. Cloned DNAs were subjected to nucleotide sequencing using the SP6 and T7 sequencing primers.

TABLE 2 List of primers used for RT-qPCR

Gene	Forward primer (5′–3′)	Reverse primer (5′–3′)
Chicken Mx	TTCACGTCAATGTCCCAGCTTTGC	ATTGCTCAGGCGTTTACTTGCTCC
Chicken GADPH	ATCAAGAGGGTAGTGAAGGCTGCT	TCAAAGGTGGAGGAATGGCTGTCA
Chicken OAS	GCAGAAGAACTTTGTGAAGTGGC	TCGGCTTCAACATCTCCTTGTACC
IBDV segment A	AAGGGCAGCTACGTCGATCTAC	TGGCAACTTCGTCTATGAAAGC

ACKNOWLEDGMENTS

We are grateful for the excellent technical assistance provided by Antonio Varas and the work of Silvia Gutiérrez-Erlandsson and Ana M. Oña from the Advanced Light Microscopy scientific CNB service. We are also extremely grateful to Gideon Schreiber for generously sharing the WT and IFNAR2-KO HeLa cell lines.

This work was supported by grants AGL2014-60095-P and AGL2017-87464-C2-1-P (AEI/FEDER, UE) to D.R. and J.F.R., L.L.C-G., E.D.-B., and D.F. were supported by predoctoral research contracts from the International Fellowship Program of the Caixa Foundation, by the FPU Program of the Spanish Ministry of Science, Innovation and Universities (FPU 18/01873), and by the Spanish Ministerio de Economía y Competitividad (BES-2015-073589), respectively. O.C.-R. was supported by a contract from the Consejería de Juventud y Deporte de la Comunidad Autónoma de Madrid (PEJD-2017-PRE/BIO-5006). The funders had no role in study design, data collection and interpretation, or the decision to submit the work for publication.

REFERENCES

1. Morrison LA, Fields BN, Dermody TS. 1993. Prolonged replication in the mouse central nervous system of reoviruses isolated from persistently infected cell cultures. J Virol 67:3019–3026. https://doi.org/10.1128/JVI.67.6.3019-3026.1993.
2. Borzakian S, Pelletier I, Calvez V, Colbere-Garapin F. 1993. Precise missense and silent point mutations are fixed in the genomes of poliovirus mutants from persistently infected cells. J Virol 67:2914–2917. https://doi.org/10.1128/JVI.67.5.2914-2917.1993.
3. Delmas D, Attoui H, Ghosh S, Malik YS, Mundt E, Vakharia VN, Ictv Report Consortium. 2019. ICTV virus taxonomy profile: *Birnaviridae*. J Gen Virol 100:5–6. https://doi.org/10.1099/jgv.0.001185.
4. van Cleef KWR, van Mierlo JT, Miesen P, Overheul GJ, Fros JJ, Schuster S, Marklewitz M, Pijlman GP, Junglen S, van Rij RP. 2014. Mosquito and Drosophila entomobirnaviruses suppress dsRNA- and siRNA-induced RNAi. Nucleic Acids Res 42:8732–8744. https://doi.org/10.1093/nar/gku528.
5. MacDonald RD, Kennedy JC. 1979. Infectious pancreatic necrosis virus persistently infects chinook salmon embryo cells independent of interferon. Virology 95:260–264. https://doi.org/10.1016/0042-6822(79)90428-8.
6. Riji John K, Richards RH. 1999. Characteristics of a new birnavirus associated with a warm-water fish cell line. J Gen Virol 80:2061–2065. https://doi.org/10.1099/0022-1317-80-8-2061.
7. van den Berg TP, Eterradossi N, Toquin D, Meulemans G. 2000. Infectious bursal disease (Gumboro disease). Rev Sci Tech Off Int Epiz 19:527–543.
8. Abdel-Alim GA, Saif YM. 2001. Detection and persistence of infectious bursal disease virus in specific-pathogen-free and commercial broiler chickens. Avian Dis 45:646–654. https://doi.org/10.2307/1592906.
9. Elankumaran RA, Heckert A, Moura L. 2002. Pathogenesis and tissue distribution of a variant strain of infectious bursal disease virus in commercial broiler. Avian Dis 46:169–176. https://doi.org/10.1637/0005-2086(2002)046[0169:PATDOA]2.0.CO;2.
10. Abdul R, Murgia MV, Rodriguez-Palacios A, Lee C-W, Saif YM. 2013. Persistence and tissue distribution of infectious bursal disease virus in experimentally infected SPF and commercial broiler chickens. Avian Dis 57:759–766. https://doi.org/10.1637/10448-110812-Reg.1.
11. Ingrao F, Rauw F, Lambrecht B, van den Berg T. 2013. Infectious bursal disease: a complex host-pathogen interaction. Dev Comp Immunol 41:429–438. https://doi.org/10.1016/j.dci.2013.03.017.
12. Delgui L, González D, Rodríguez JF. 2009. Infectious bursal disease virus persistently infects bursal B-lymphoid DT40 cells. J Gen Virol 90:1148–1152. https://doi.org/10.1099/vir.0.008870-0.
13. Baba TW, Giroir BP, Humphries EH. 1985. Cell lines derived from avian lymphomas exhibit two distinct phenotypes. Virology 144:139–151. https://doi.org/10.1016/0042-6822(85)90312-5.
14. Cubas-Gaona LL, Diaz-Beneitez E, Ciscar M, Rodríguez JF, Rodríguez D. 2018. Exacerbated apoptosis of cells infected with infectious bursal disease virus upon exposure to interferon alpha. J Virol 92:e00364-18. https://doi.org/10.1128/JVI.00364-18.
15. Aaronson DS, Horvath CM. 2002. A road map for those who don't know JAK-STAT. Science 296:1653–1655. https://doi.org/10.1126/science.1071545.
16. Santhakumar D, Rubbenstroth D, Martinez-Sobrido L, Munir M. 2017. Avian interferons and their antiviral effectors. Front Immunol 8:49. https://doi.org/10.3389/fimmu.2017.00049.
17. Reboul J, Gardiner K, Monneron D, Uzé G, Lutfalla G. 1999. Comparative genomic analysis of the interferon/interleukin-10 receptor gene cluster. Genome Res 9:242–250.
18. Piehler J, Thomas C, Garcia KC, Schreiber G. 2012. Structural and dynamic determinants of type I interferon receptor assembly and their functional interpretation. Immunol Rev 250:317–334. https://doi.org/10.1111/imr.12001.
19. Zhao W, Lee C, Piganis R, Plumlee C, de Weerd N, Hertzog PJ, Schindler C. 2008. A conserved IFN-alpha receptor tyrosine motif directs the biological response to type I IFNs. J Immunol 180:5483–5489. https://doi.org/10.4049/jimmunol.180.8.5483.
20. Urin V, Shemesh M, Schreiber G. 2019. CRISPR/Cas9-based knockout strategy elucidates components essential for type 1 interferon signaling in human HeLa cells. J Mol Biol 431:3324–3338. https://doi.org/10.1016/j.jmb.2019.06.007.
21. O'Brien MA, Moravec RA, Riss TL. 2001. Poly(ADP-ribose) polymerase cleavage monitored in situ in apoptotic cells. Biotechniques 30:886–891. https://doi.org/10.2144/01304pf01.
22. Kane M, Golovkina T. 2010. Common threads in persistent viral infections. J Virol 84:4116–4123. https://doi.org/10.1128/JVI.01905-09.
23. Martín Hernández AM, Carrillo EC, Sevilla N, Domingo E. 1994. Rapid cell variation can determine the establishment of a persistent viral infection. Proc Natl Acad Sci U S A 91:3705–3709. https://doi.org/10.1073/pnas.91.9.3705.
24. Grundhoff A, Sullivan CS. 2011. Virus-encoded microRNAs. Virology 411:325–343. https://doi.org/10.1016/j.virol.2011.01.002.
25. Manzoni TB, López CB. 2018. Defective (interfering) viral genomes re-explored: impact on antiviral immunity and virus persistence. Future Virol 13:493–503. https://doi.org/10.2217/fvl-2018-0021.
26. Valdovinos MR, Gómez B. 2003. Establishment of respiratory syncytial virus persistence in cell lines: association with defective interfering particles. Intervirology 46:190–198. https://doi.org/10.1159/000071461.
27. Stetson DB, Medzhitov R. 2006. Type I interferons in host defense. Immunity 25:373–381. https://doi.org/10.1016/j.immuni.2006.08.007.
28. Burkhardt E, Muller H. 1987. Susceptibility of chicken blood lymphoblasts and monocytes to infectious bursal disease virus (IBDV). Arch Virol 94:297–303. https://doi.org/10.1007/BF01310722.
29. Inoue M, Yamamoto H, Matuo K, Hihara H. 1992. Susceptibility of chicken monocytic cell lines to infectious bursal disease virus. J Vet Med Sci 54:575–577. https://doi.org/10.1292/jvms.54.575.
30. Subissi L, Keita M, Mesfin S, Rezza G, Diallo B, Van Gucht S, Musa EO, Yoti Z, Keita S, Djingarey MH, Diallo AB, Fall IS. 2018. Ebola virus transmission caused by persistently infected survivors of the 2014-2016 outbreak in West Africa. J Infect Dis 218:S287–S291. https://doi.org/10.1093/infdis/jiy280.
31. Ostertag D, Hoblitzell-Ostertag TM, Perrault J. 2007. Overproduction of double-stranded RNA in vesicular stomatitis virus-infected cells activates a constitutive cell-type-specific antiviral response. J Virol 81:503–513. https://doi.org/10.1128/JVI.01218-06.

32. Méndez F, de Garay T, Rodríguez D, Rodríguez JF. 2015. Infectious bursal disease virus VP5 polypeptide: a phosphoinositide-binding protein required for efficient cell-to-cell virus dissemination. PLoS One 10: e0123470. https://doi.org/10.1371/journal.pone.0123470.
33. Albar JP, Fernández-Arias A, Martínez S, Rodríguez JF, Risco C. 1998. Expression of ORF A1 of infectious bursal disease virus results in the formation of virus-like particles. J Gen Virol 79:1047–1054. https://doi.org/10.1099/0022-1317-79-5-1047.
34. Soubies SM, Courtillon C, Briand FX, Queguiner-Leroux M, Courtois D, Amelot M, Grousson K, Morillon P, Herin JB, Eterradossi N. 2017. Identification of a European interserotypic reassortant strain of infectious bursal disease virus. Avian Pathol 46:19–27. https://doi.org/10.1080/03079457.2016.1200010.
35. Li H, Durbin R. 2009. Fast and accurate short read alignment with Burrows-Wheeler transform. Bioinformatics 25:1754–1760. https://doi.org/10.1093/bioinformatics/btp324.
36. Li H, Handsaker B, Wysoker A, Fennell T, Ruan J, Homer N, Marth G, Abecasis G, Durbin R, 1000 Genome Project Data Processing Subgroup. 2009. The Sequence Alignment/Map format and SAMtools. Bioinformatics 25:2078–2079. https://doi.org/10.1093/bioinformatics/btp352.
37. Wang K, Li M, Hakonarson H. 2010. ANNOVAR: functional annotation of genetic variants from high-throughput sequencing data. Nucleic Acids Res 38:e164. https://doi.org/10.1093/nar/gkq603.